OFFSHORE STRUCTURES FOR AQUACULTURE. COMPARISON OF ANALYSIS WITH MODEL TESTING

Are Johan Berstad
Dr. Ing. President Aquastructures, Norway.
www.aquastructures.no,
Email: are@aquastructures.no

Jan Vidar Aarsnes
Dr. Ing. Vice president CeFront, Norway
www.CeFront.no
Email: jva@cefront.no

ABSTRACT

This paper presents how structures similar to structures used offshore by the oil and gas industry now due to governmental regulations are introduced to the fishfarming industry.

One of the new offshore concepts in the "AquaTraz. Model testing have been applied on this concept and results from the model test is compared with AquaSim analysis. In general results correspond well. The respons deviating from classic fish farms is shown and what extra considerations that should be carried out for this type of systems compared to classic fish farms is discussed.

INTRODUCTION

The aquaculture industry in Norway has increased rapidly the last decades. In the early years the industry was regulated only under the laws for free enterprise until the first specific laws were put into place in 1973. Since then rules and regulations have evolved and in 2003 the design code NS 9415 was introduced, establishing design criteria. In 2009, the Norwegian standard, NS 9415 was revised and in 2011 corresponding regulations were enforced. Structural integrity to defined load criteria had to be documented. This largely increased the engineering effort within the industry and as more systems were assessed and documented to this regime, the number of escaped fish plummeted.

In 2015 development concessions (utviklingstillatelser) were introduced. This basically meant that in order to increase the production from fishfarming some kind of novel concept had to be introduced. This has lead to a large increase in novel concepts ranging fully submerged flexible units to classic offshore structures used for fishfarming.

In addition, recent years have seen the introduction of other innovations such as "lice skirts" leading the structural response to be more mass dominated than drag dominated response of classic net based units which was the dominating design when NS 9415 was introduced in 2003 and revised in 2009.

90% of the fish farms in norway are based on polyethylene floating collars with a flexible ned underneath as shown Figure 1.
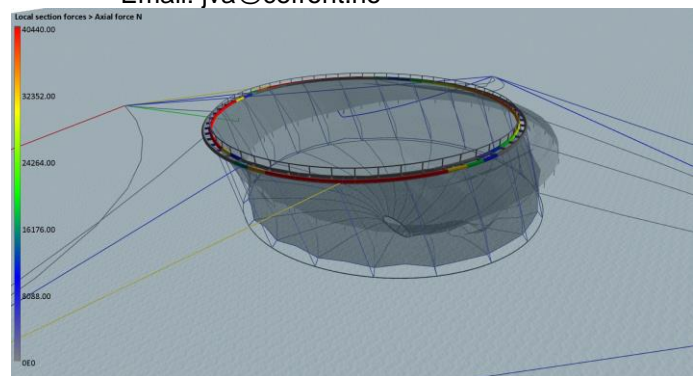

Figure 1 Net in floating collar

Figure 1 shows a net with an impermeable lice skirt in the upper part of the net. The net cages are normally laid out in a grid like the one shown in Figure 2.
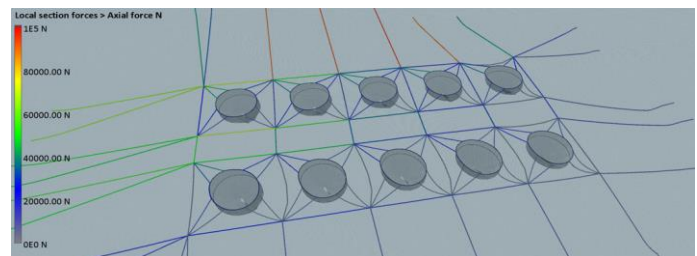

Figure 2 Grid system

The first development concessions were granted to the "Ocean farm" operated by Salmar (Figure 3). In this system a permeable net is spread out within a steel frame.

Figure 3 The Salmar concept "Ocean farm"

The Ocean farm was also the first applicant. It was applied for 104 concepts before the closure date. Most are being processed while a few have been granted concessions.

Jan Vidar på AquaTraz, legger inn.

THE AQUATRAZ CASE STYDY

This report outlines a comparison between analysis and model testing of the AquaTraz fish farm cage seen in Figure 4.

Figure 4 AquaTraz fish farm

This paper presents the theoretical basis of the analysis, the test tank model and the analysis made of the tested system.

THEORETICAL BASIS FOR THE ANALYSIS PROGRAM AQUASIM

The AquaSim program is based on the finite element method. It utilize beam and shell elements with rotational DOF's, as well as membrane elements and truss elements with no rotational stiffness. Geometric nonlinearities are accounted for in all element types, such that the program handles large structural deformations. The program is based on time domain simulation where it is iterated to equilibrium at each time instant. Both static and dynamic time domain simulation may be carried out. Features such as buoys, weights, hinges and springs are included in the program

The basic idea of the FE analysis program is to establish equilibrium between external loads acting on the structure at a given time instant and internal reaction forces.

$$\sum F = \mathbf{R}_{ext} + \mathbf{R}_{int} = 0$$

Equation 1

where R_{ext} is the total of the external static forces acting on the structure at a given time instant and R_{int} is the internal forces. The structure is discretized to a finite number of degrees of freedom (DOF's). Equation 1 is then discretized as

$$F^{idof} = \mathbf{R}_{ext}^{\ idof} + \mathbf{R}_{int}^{\ idof} = 0, \quad idof = 1, N_{dof}$$

Equation 2

where N_{dof} is the discrete number of DOF's the structure has been discretized into. The current element program deals with strongly nonlinear behavior both in loads and structural response. In order to establish equilibrium, the tangential stiffness method is used. External loads are incremented to find the state of equilibrium. Having established equilibrium in time step *i-1*, the condition for displacement *r*, step *i*, is predicted as

$$\Delta \mathbf{R}^i(\mathbf{r}_{i-1}) = \mathbf{R}_{ext}^{\ i}(\mathbf{r}_{i-1}) + \mathbf{R}_{int}^{\ i-1}(\mathbf{r}_{i-1}) = \mathbf{K}_t^{i-1}\Delta \mathbf{r}$$

Equation 3

where K_t^{i-1} is the tangential stiffness matrix at configuration *i-1*. The external load is calculated based on the configuration of the structure at *i-1*. This gives a prediction for a new set of displacements *(j=1)*. Based on Equation 3, a prediction for the total displacement $r_{(j=1)}$, is found as

$$\bar{\mathbf{r}}_{j=1} = \mathbf{r}_{i-1} + \Delta \mathbf{r}$$

Equation 4

Based on this estimate for new displacements, both external and internal forces are derived based on the new structural geometry and the residual force, *ΔR* is put into the equation of equilibrium as follows

$$\Delta \mathbf{R}(\bar{\mathbf{r}}_j) = \mathbf{R}_{ext}^{\ i}(\bar{\mathbf{r}}_j) + \mathbf{R}_{int}^{\ i}(\bar{\mathbf{r}}_j) = \mathbf{K}_t^{\ i}\Delta \mathbf{r}$$

Equation 5

Note that both the external and internal forces will vary for each iteration due to the strongly hydroelastic nature of the fluid structure interaction. Equation 5 is solved for the displacement *Δr*. Incrementing *j* with one, the total displacement is now updated as

$$\bar{\mathbf{r}}_j = \bar{\mathbf{r}}_{j-1} + \Delta \mathbf{r}$$

Equation 6

Now if Δr found from Equation 5 is larger than the tolerated error in the displacements, Equation 4 is updated *(j = j+1)* and Equation 5 is solved based on the new prediction for displacements, this is repeated until, *Δr* is smaller than a tolerated error, then

$$\mathbf{r}_i = \bar{\mathbf{r}}_j$$

Equation 7

i is increased with one, and Equation 4 is carried out for the new load increment.

At the default configuration, the program works as this: Static analysis is used to establish static equilibrium including buoyancy. Secondly, current loads are applied then wind and wave loads are added. (Still static analysis). Then dynamic analysis commence. Waves are introduced with the first wave used to build up the wave amplitude. Both regular waves and irregular waves may be simulated. Waves are assumed to be sufficiently described by linear wave theory. Inertia and damping are accounted for in the wave analysis, meaning that mass and damping are accounted for in the equations of equilibrium. The Newmark-Beta scheme is applied for the dynamic time domain simulation (e.g. Langen and Sigbjørnson 1979). Note that the above equations imply using the Euler angles for rotations. This is just a simplification for easy typing. For rotational DOF´s Aquasim uses a tensor formulation for the rotations as outlined in e.g. Eggen (2000) which should be applied to handle 3D rotations in an appropriate manner.

Wave loads may be derived using the Morison formulae (Morison et al 1950) or using diffraction theory.

AquaSim utilize different tequiques for finding diffraction forces. To find forces on the impermeable tank in this case, numerical 3D source tequique as described by Babarit and Delhommeau (2015) and verification assessment is described in Parisella and Gourlay (2016). When numerical analysis is applied for diffraction forces, also added mass and damping from wave generation is found by the same numerical tequique with the option to scale the added mass effect in AquaSim. Added mass and damping are derived for the steady state position and the kept unchanged. Diffraction forces are calculated at the actual position and with the systems actual deformation. Linearized values for diffraction, added mass and damping are derived for the elements mean wetted position. For irregular waves, linearized added mass and damping for the characteristic period in the wave spectrum are used in the calculations. Wave interaction between separate components is not accounted for.

For elements where the Morison formulae is applicable, the cross flow principle is applied for beams and truss elements (see. e.g. Faltinsen 1990). The drag load term of this equation is quadratic with respect to the relative velocity between the undisturbed fluid and the structure, both the mass of the structure as well as added mass in the cross sectional plane is accounted for. Due to the large deflections occurring, the added mass is nonlinear. For nets the method presented by Berstad et. al. (2012) is applied. A main difference in the drag load to nets compared with drag loads to lines in the increase of the drag due to the presence of the net. Berstad et al (2012) formulated this as an increased drag coefficient

$$Cd_{mem} = Cd_{cyl} \frac{1}{(1 - \frac{Sn}{2})^3}$$

Equation 8

Where Sn is the solidity of the net.

A further description of load and response for permeable nets in AquaSim see e.g. Aquastructures (2018) or Berstad et. al. (2012)

AquaSim has undertaken a versatile verification scheme: Analysis has been carried out on a wide range of computational cases where results have been compared to handbook formula or other programs, see Aquastructures (2012). Tank testing has been carried out and compared to analysis, see Berstad et al (2004). The program has been compared to accidents where the capsize origins were known (Aquastructures 2003 and 2005). In addition experience have been obtained during several years where the program has been the most used program for calculation of the structural integrity of fish farm systems in Norway. These systems in general consist of moorings, structure and nets responding to wave and current in a strongly hydroelastic manner. The program is also used for a wide range of offshore applications such as towing for seismic operations (Berstad and Tronstad 2008), operations and installations offshore, mooring analysis of offshore units and structural and mooring analysis of equipment for renewable equipment offshore (see e.g. Berstad et. al. 2007)

MODEL TEST

Model basin testing have been carried out for the fish farming cage seen in Figure 5. The testing was carried out at Sintef Ocean (Sintef 2017). The test tank model is shown in Figure 5.

Figure 5 Test tank model.

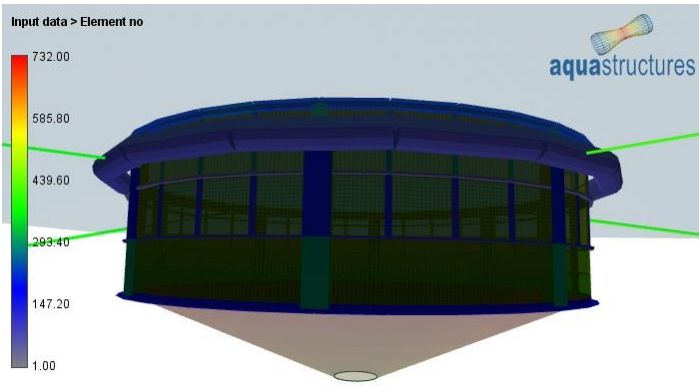The AquaSim analysis model is made in full scale coordinates and is shown in Figure 6.

Figure 6 Analysis model. Element discretization.

The cage including floater is a steel cage where the upper 9.6 meters of the cage is impermeable steel. The net cage is built has main particulars given in Table 1.

Table 1 Main particulars floater.

Main particulars cage	Analysis model	Tank model (full scale values)
Freeboard in still water [m]	2.223	2.235
Scale factor	1	15
Type of scale		Froude
Diameter main cage [m]	51	51
Diameter floating collar at water line [m]	2.4	2.4
Horizontal distance from tank[m] center floater at knuckle points	27.8	
Total height vertical part [m]	14.6	14.6
Vertical centre of gravity [m] (from baseline)	9.72	9.75
Weight of system [Tonnes]	598	597
Vertical height conical part of net [m]	10.1	10.1
Net solidity [%]	23	23
Scale factor net mesh		1
Weight in water bottom cone [kg]	800	800

Two versions of the cage cave been tested. The difference between them is the lower part of the wall sided tank, the areas seen transparent in Figure 7 denoted "Lower vertical net". Two versions were tested. The model configuration denoted "Base" where this net was impermeable and the configuration "Alt 1" where this net was permeable. Both these cases have been modeled and results have been compared.
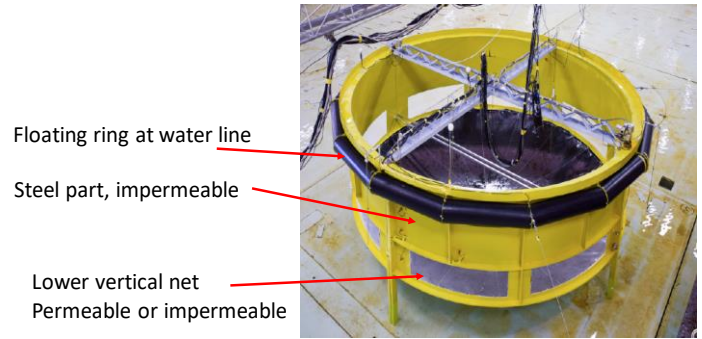

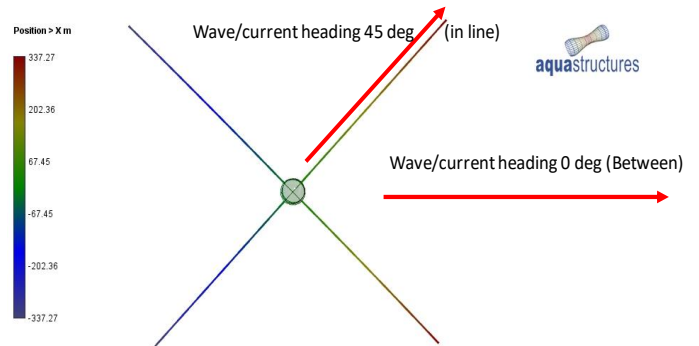**Figure 7 Two versions "Base" with impermeable vertical net and "Alt 1" with permeable net (solidity 23%)**

Figure 8 Mooring system with definition of wave an current direction. This paper compares current both with 0 and 45 degrees. For waves and waves including current all directions are 0 degrees meaning the wave propagation direction is in between the mooring lines with a symmetry plane.

The main particulars for the mooring system are given in Table 2.

Table 2 Main particulars for mooring system.

Main particulars mooring system	Analysis model	Tank model (full scale values)
Length of each mooring line	450	>280
Axial stiffness of each mooring line [kN/m]	30	30
Elastic module of each mooring line, EA [kN]	13524	
Pretension [kN]	500	500

The mooring system is such that it keeps the main response of the system linear within the tested load levels. The stiffness of the mooring system was set equal to the stiffness in the tested model at 60 kN/m. As shown in Figure 9 the pretension both in the test and in the analysis is 500 kN.
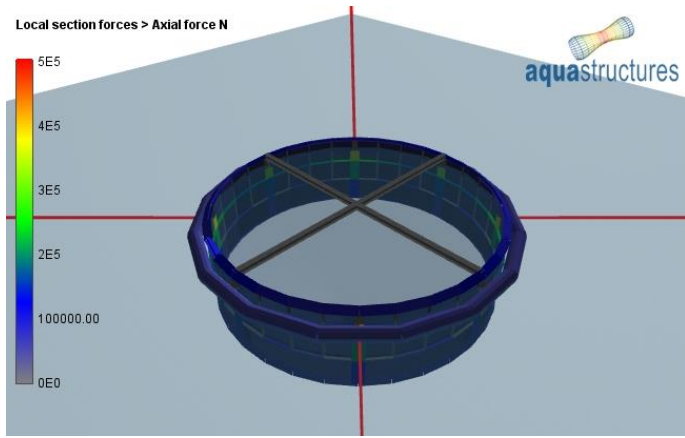
4   Copyright © 2014 by ASME

Figure 9 Pretension 500 kN

Figure 10 shows the tangential stiffness of the analysis model. This compares to the model.
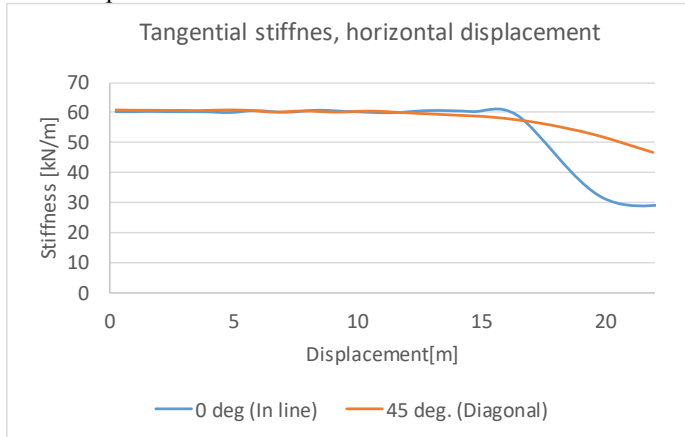

Figure 10 Tangetial stiffness of the system

The analysis model has been established with the default parameters most commonly. Pressure due to current have been calculated by the default formulation in AquaSim (see e.g. Aquastructures 2018) where a drag coefficient is given to the large volume structure and pressures is applied such that the force in total corresponds to the drag coefficient multiplied with the projected area being diameter * height.

Response from current
The 3 cases shown in Table 3 have been tested in the tank with current and no waves.

Table 3 Test cases current

Test no	Cage condition	Heading	U_C [m/s]
1310	Base	0 deg	0.732
1320	Base	45 deg	0.697
1330	Alt. 1	0 deg	0.727

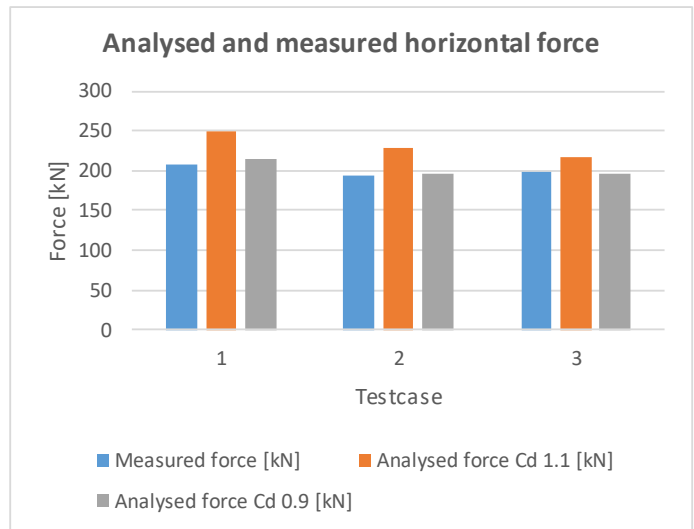Figure 11 shows comparison between analysis and measurements.

Figure 11 Analysis compared with measurements for current

As seen from Figure 11 calculated results with the base drag coefficient of 1.1 are slightly conservative whereas when the drag coefficient is reduced to 0.9 there is good correspondence. This is in line with what was observed during testing that the water flowed more underneath the cage than along the sides. This is natural since that diameter is larger than the draught.

Decay test and added mass
Decay testing was carried out and results are shown in Figure 12. Decay testing was carried out for the "Base" model only.

First the decay test was used to investigate the amount of added mass the system is subjected to both from fluid inside the tank and outside the tank. As seen from Figure 12 the period of the system is approximately 130 seconds. The internal and external added mas was chosen to fit this. This means that the added mass was set to be 19E6 kg which is slightly less than half (41%) of the internal mass and the added mass. This was used for the succeeding analysis. The reason not all inside mass contributes as added mass is probably that the diameter is approx. 5 times larger than the drought which means water is flowing underneath. This is probably also the case for the outside added mass.
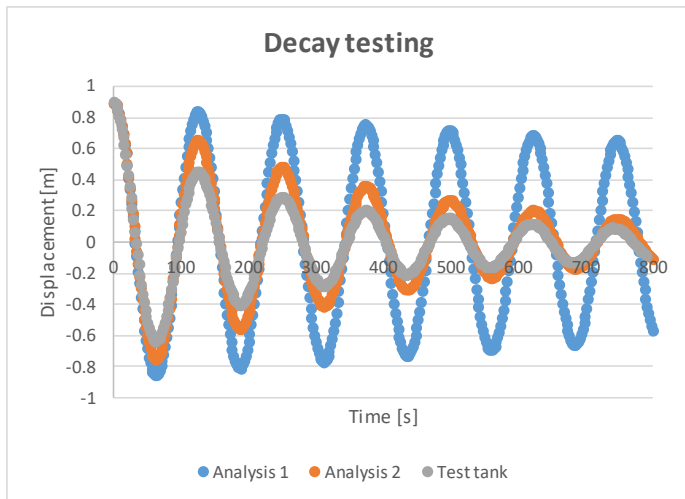
Figure 12 Decay test analysis compared to testing

Two versions of the analysis are compared with the testing

- Analysis 1 is the analysis model with default drag coefficients and no extra damping.
- In Analysis 2 damping of 0.3 % if the mass in the tank including added mass from water is added as a linear damping coefficient.

As seen from Figure 9 the decay is a lot slower if only damping from drag loads based on the drag coefficients used in the analysis is applied. If a linear damping coefficient of 0.3% of the mass in applied decay is in the same range. In real life it is probably other and local damping effects causing the increased decay such as vortices trough sharp corners, wave generation or damping in measurement cabling and system.

Regular wave

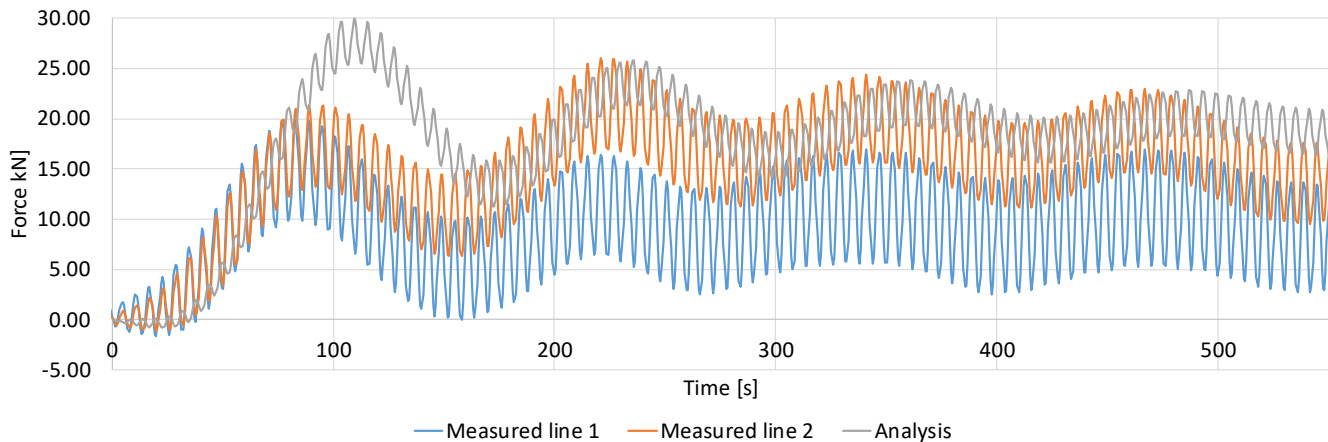A regular wave with wave height 0.97 meters and period 6 seconds is compared in Figure 13. There is no current.

Figure 13 Regular wave amplitude 0.485 m , period 6 seconds. Axial force in mooring line 1 and 2. (symmetric in the analysis).
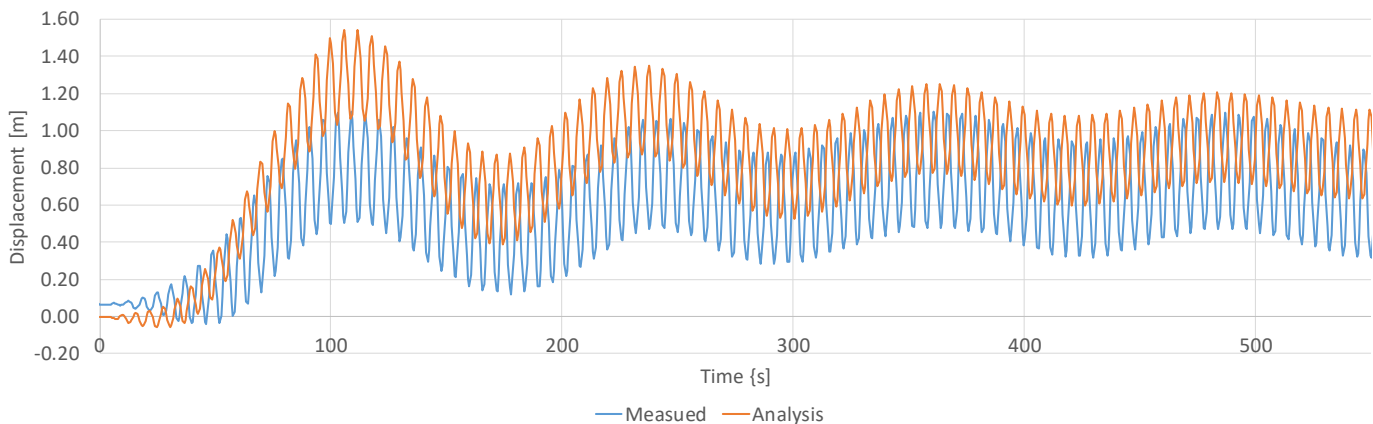

Figure 14 Regular wave amplitude 0.485 m , period 6 seconds. Displacement centre of ring.

The analysis shown in Figure 13 and Figure 14 have been carried out with default drag settings. In and out of water and

wave drift is accounted for in the analysis. The drift forces to the main cylinder in the analysis are calculated by keeping the 2nd order terms giving a nonzero mean, the pressure all the way to the water line

$$p = -\rho g \int_0^\zeta z\, dz - \rho \frac{\partial \varnothing_1}{\partial t}\Big|_{z=0}\zeta$$

Equation 9

Note that the wave elevation is accounted for also below the mean water line so that the total pressure is not allowed to be less than 0. and:

$$-\frac{\rho}{2}\int_{-\infty}^{0}\left\{\left(\frac{\partial\phi_1}{\partial x}\right)^2+\left(\frac{\partial\phi_1}{\partial y}\right)^2+\left(\frac{\partial\phi_1}{\partial z}\right)^2\right\}dz$$

Equation 10

which is the velocity term in Bernoullis equation. In case the wave field rides on top of a mean current velocity, the calculated drift force is adjusted with the term:

$$F_2 = F_2(1+\frac{\omega U Cos\beta}{g})$$

Equation 11

where F_2 denotes that these are 2nd order load effects where F2 is the sum of The term in the above equation is only added for the part of the pressure above mean water line as is connected for F_2.

Irregular waves
Figure 7 shows the 3 irregular wave conditions considered.

Table 4 irregular wave conditions considered

Test	Hs	Tp	Curvel	Direction
3221	1.7	5.2	0	0
3240	2.8	6.8	0	0
3260	2.8	6.8	0.72	0

Figure 15 shows statistical key parameters for test case 3221.

- Analysis: Calculated by numerical analysis. 20 minuts calculation. The wave spectrum is subdivided to 100 individual waves and the mean period of each wave block is chosen randomly in the interval between the lowest and the highest wave in the block. The same random sees has been used for alle base analysis cases for the conditions in Table 4. For further information on this see e.g. Aquastructures (2018)
- Measured 20 min 1. Measured first 20 minutes
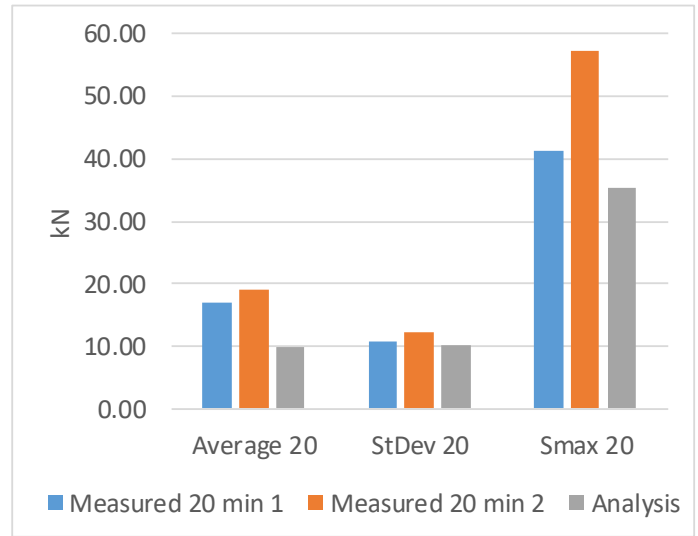- Measured 20 min 2. Measured second 20 minutes i.e 20 min to 40 minuts into the time series.

Figure 15 Comparison analysis and measurements testcase 3221. Axial force line 1

Figure 16 shows the same as Figure 16 but in this case the cetre point of the system is compared. The trend is the same but the standard deviation of the analysis and the first 20 minutes of the test is even more similar.
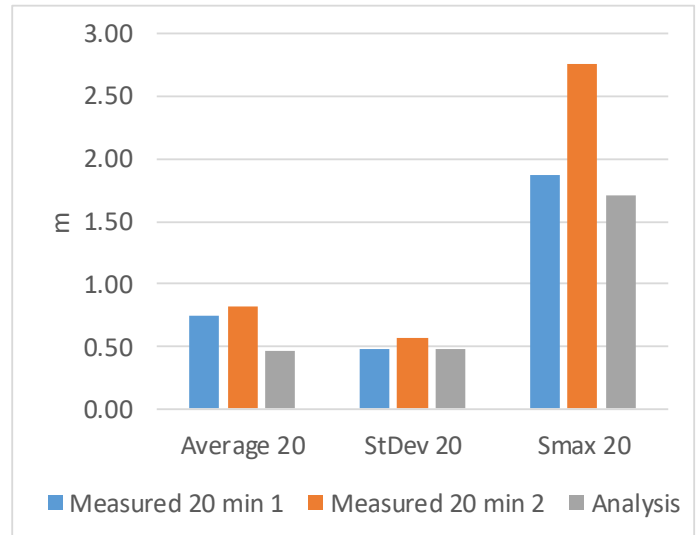

Figure 16 17 Comparison analysis and measurements testcase 3221. Displacement centre point of cage.

Figure 18 shows the time series of the analysis compared with the two first 20 minutes periods of the testing. As seen from the figure it is the drift of the system related to the eigenperiod for horizontal motion of the system. This documents the importance of accounting for this when changing from normal drag dominated systems to mass dominated system that this cage is. Note that the eigenperiod of the system for the case Alt 1 is lower than the Base case due to permeable net. For the analysis, the eigenperiod is 93 seconds which seem to correspond well with the test which looks to be in the +- 100 range based on visual inspection of Figure 18.
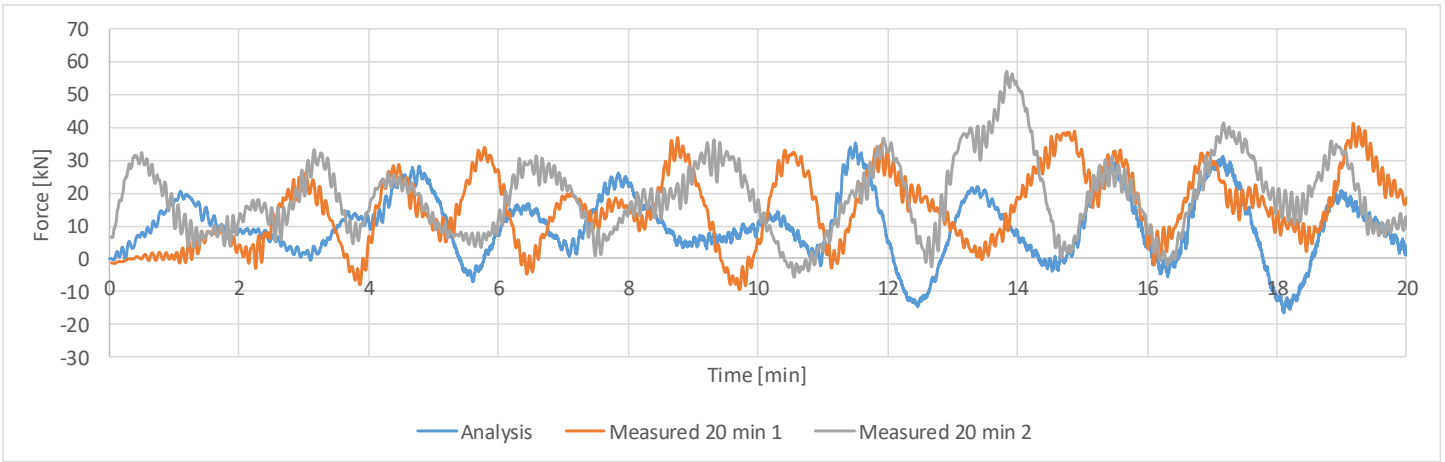
Figure 18 Comparison analysis and measurements testcase 3221. Axial force mooring line 1. Time series 20 minutes excerps

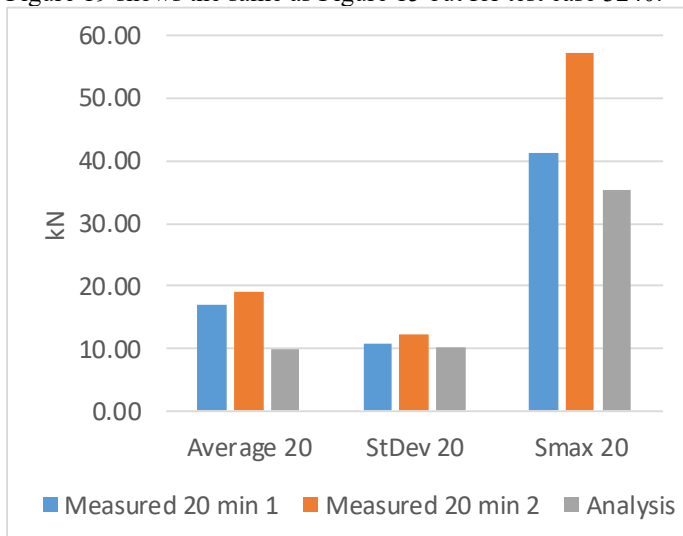Figure 19 shows the same as Figure 15 but for test case 3240.

Figure 19 Comparison analysis and measurements testcase 3240. Axial force line 1

Figure 19 shows the same trend as Figure 15 meaning that the average drift is underpredicted by the analysis whereas the standard deviation corresponds well.

Figure 20 shows the time series of the analysis compared with the two first 20 minutes periods of the testing. Also in this case the drift of the system related to the eigenperiod for horizontal motion of the system dominates the response.
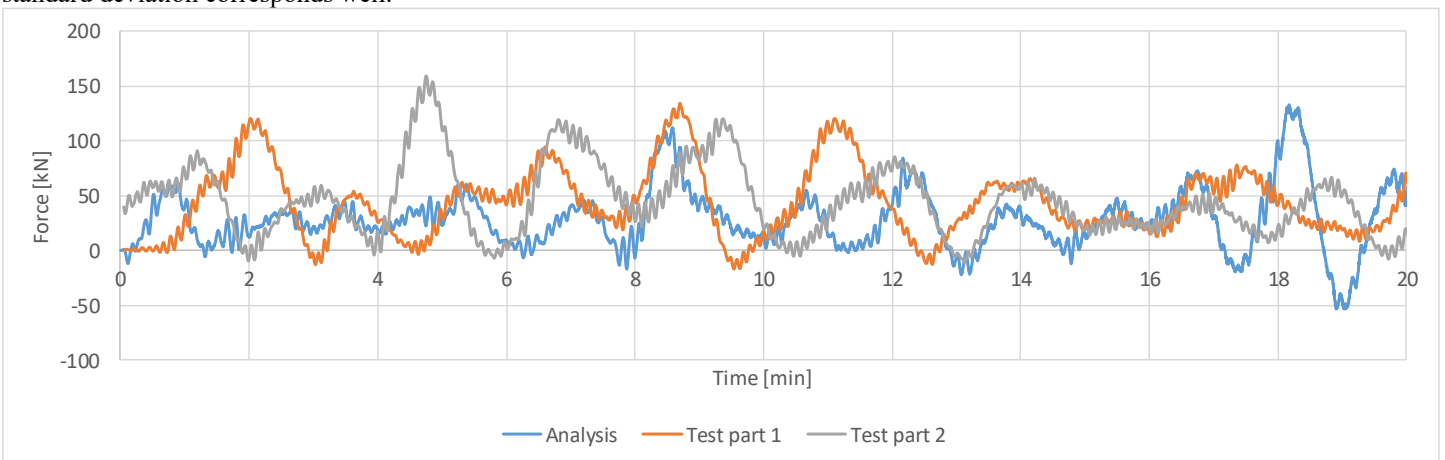

Figure 20 Comparison analysis and measurements testcase 3240. Axial force mooring line 1. Time series 20 minutes excerps

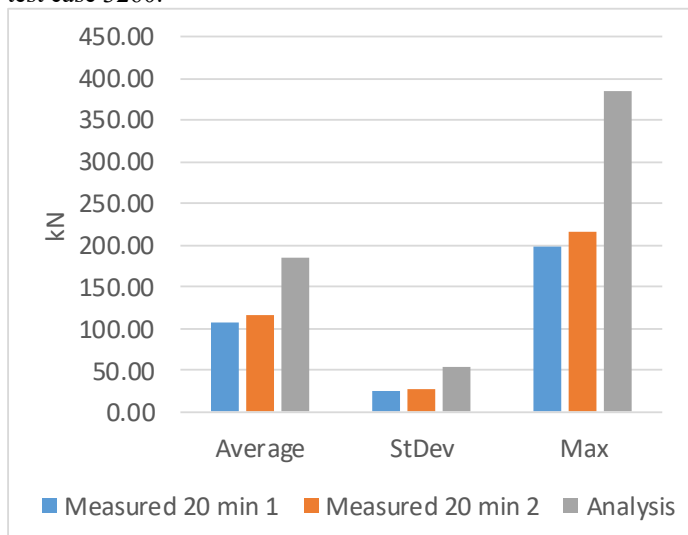Figure 21 shows the same as Figure 15 and Figure 19 but for test case 3260.

Figure 21 Comparison analysis and measurements testcase 3260. Axial force line 1

As seen from Figure 21 both the mean value, the standard deviation and the maximum are larger in the analysis. Figure 22 compares:

- Measured 3 hours: Statistical values for the full 3 hour tank test
- Analysis: The base analysis referred to in Figure 21.
- Analysis 2: same as analysis but with another random seed.

- Analysis 3: Same as analysis, but in this case the wave periods has been set to the middle wave period instead of randomization within the interval.
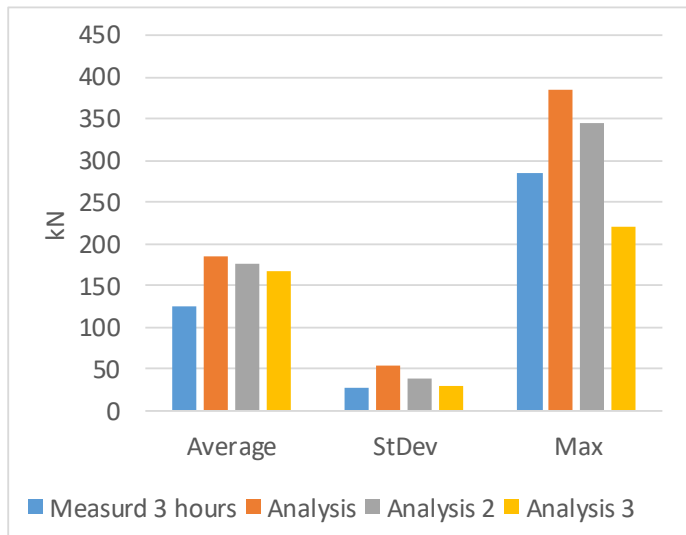

Figure 22 Statistical values for the full 3 hour test compared to 3 analysis realizations.

As seen from Figure 21 and Figure 22 the analysis shows in general larger response than the measurements for this case. Note how dependent the response is to weather the period of the individual waves is randomized or not. Tme series are seen in Figure 23.
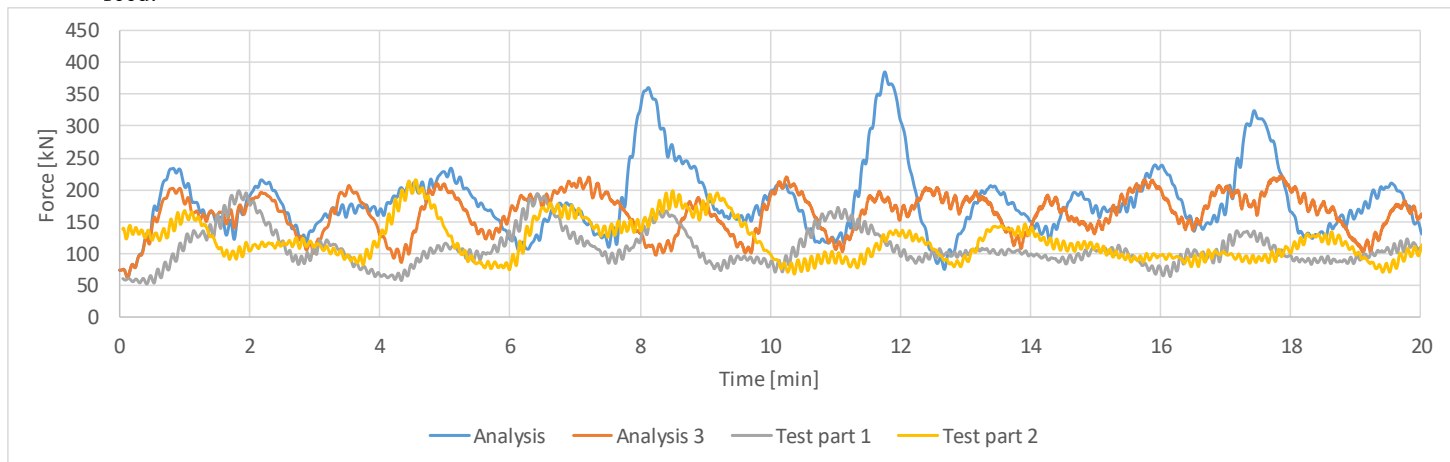

Figure 23 Comparison analysis and measurements testcase 3260. Axial force mooring line 1. Time series 20 minutes excerps

as seen from the time series the analysis with randomized peaks have some additional peaks compared with the nonrandomized. This means on should be careful when performing irregular analysis such that one manage to obtain the relevant statistical maximum.

DISCUSSION

Figure 24 shows a comparison of average axial force in line 1 for load case 3260 compared with the axial force in line 1 for

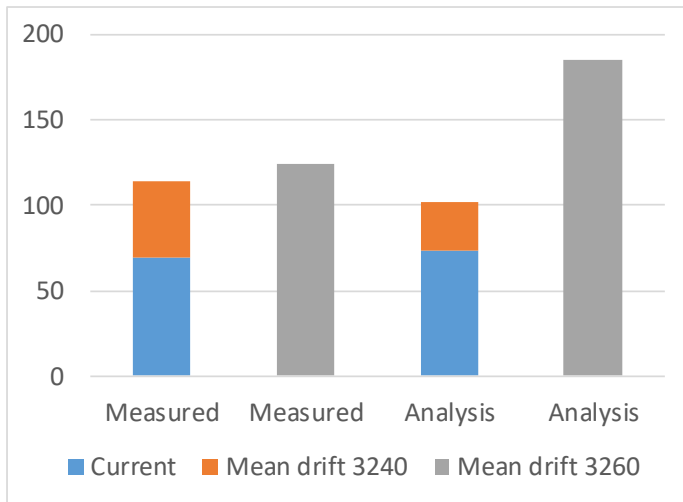the load case with current only, 1330 and mean drift for load case 3240.

Figure 24 Comparison analysis and measurements testcase 3260. Axial force line 1. Current condition 1330, waves conditions 3240 and 3260.

As seen from Figure 24, the mean drift for load case 3260 is approximately 10% larger than the current response in load case 1330 plus the mean drift for load case 3240. The analysis shows a difference of 60-80%. depending on the realization.

Consider a fixed vertical cylinder with only the drag part of the Morison equation acting. The force acting on this cylinder will then be caused by the horizontal current and the horizontal part of the velocity caused by waves.

En excerpt of the horizontal water particle velocity is shown in Figure 25. As seen, when the waves are assumed to ride upon the curren field, the average horizontal water particle velocity will shift from 0 average to the current velocity as average.
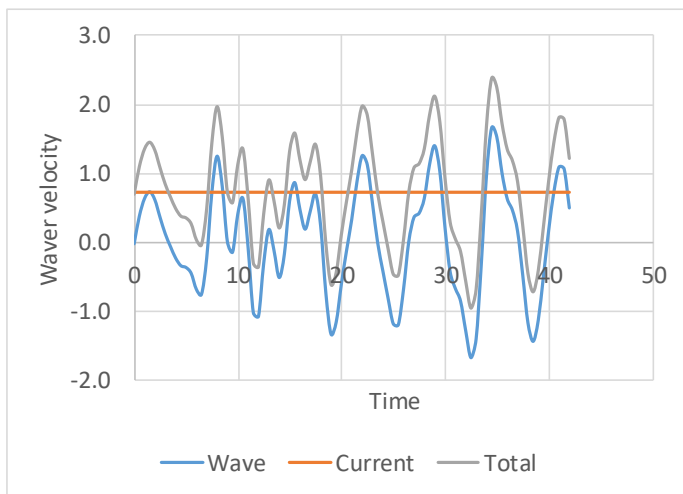

Figure 25 Excerpt of horizontal particle velocity at the water line for test 3260.

As shown in Figure 26 this will make an average quadratic force larger than the current velocity. Introducing relevant number for the present case this will increase the average drag force approximately 35-40 %. In addition the wave drift force will increase slightly less than 10%. This means one should

expect the difference in the mean force to higher than what the test results show.
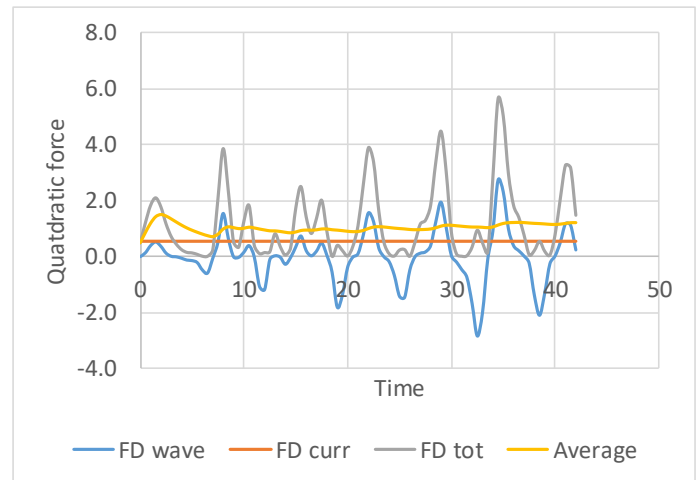

Figure 26 Quadratic force average increase due to combination of current and wave

Figure 27 shows the first minute of measurements and analysis for case 3260. It could be that increasing the waves in the tank leads to a reduced mean current. As seen from the figure, the loads stay for a while in the range og 50-60 kN. This means that the effective current is lower than the original measurement. This may be a cause for the highet combined drift both in the analysis and in the theorethical consideration.
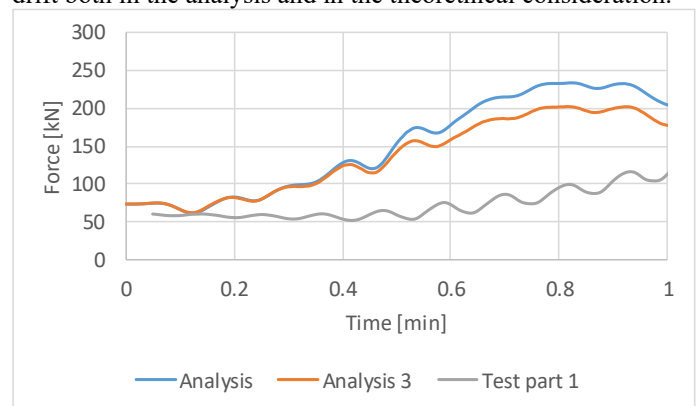

Figure 27 First minute of test and analysis case 3260. Axial force in line 1.

APPLICATION FOR ENGINEERING
For engineering for fishfarming one would like a fast but conservative base method and in addition open up for more refined analysis and even more refined a combinations of analysis and model testing.

Figure 28 shows response from regular wave with wave height = 1.9*Hs both for Peak period of the spectrum and for the corresponding Tz of the spectrum. According to NS 9415 one should use H = 1.9*Hs if one carries out analysis according to NS 9415 whereas now many waves to analyse is not specified. The culture for regular drag dominated fish farms is to apply one wave to build the full wave amplitude, then analyse with one or two extra waves.
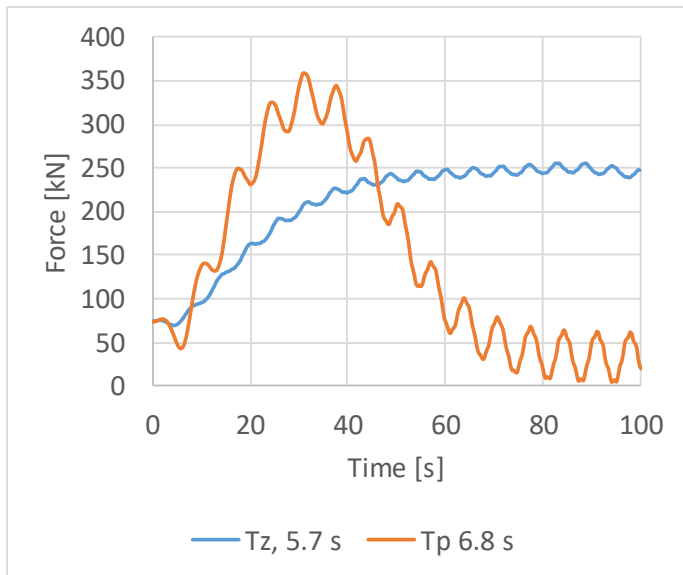
10   Copyright © 2014 by ASME

Figure 28 Response from regular wave

As seen from Figure 28 the response pattern is very different for the two cases. The response with wave period = Tp give a highr response then the system comes back and what looks to be some coupled response, the system comes back. The response at wave period Tz is different using longer time to find the maximum and then not pushing back in the same manner. What is seen is that passing a timelength of less than half of the eigenperiod for the system one obtains a maximum that is larger than the max response for the irregular wave. This means that a valid analysis approach can be to use regular waves but then use time series which is as long as half the eigenperiod.

Note that finding an appropriate eigenperiod is not as easy for a real case than for this model test case. For a real case, the eigenperiod will vary strongly from the load condition. In general, the more current the lower eigneperiod, and it there is no current, the eigenperiod is so large that in real life, the systems respondes, and then any resonant behaviour fades out at it comes back towards zero displacement. The eigenperiod with current is the relevant eigenperiod to determine the length of the analysis.

CONCLUSIONS

From the comparison between analysis and measurements the following can be concluded:
- Analysis compares very well to test data within the accuracy level limited by the scope of measurements.
- Both analysis and testing confirms that mass dominated fish farms leads to some extra assessment needed for response calculation. One must make sure to include 2nd order wave effects leading to wave drift forces in the analysis.
- For design it is load conditions with wave and current combined that is relevant. For these conditions, the analysis are shown to be conservative as long as the wave train realization is built up with randomized periods.
- The randomization leads to a range in response parameters. One must ensure to run long enough time series to obtain statistical validity of peak response.

- In order to ensure large enough response by doing analysis with regular waves one should run past half of the eigenperiod.
- Doing further measurements one should preferably log current at more locations.

ACKNOWLEDGMENTS

APPENDIX 1

This appendix adds some further description of the test model and the analysis model.
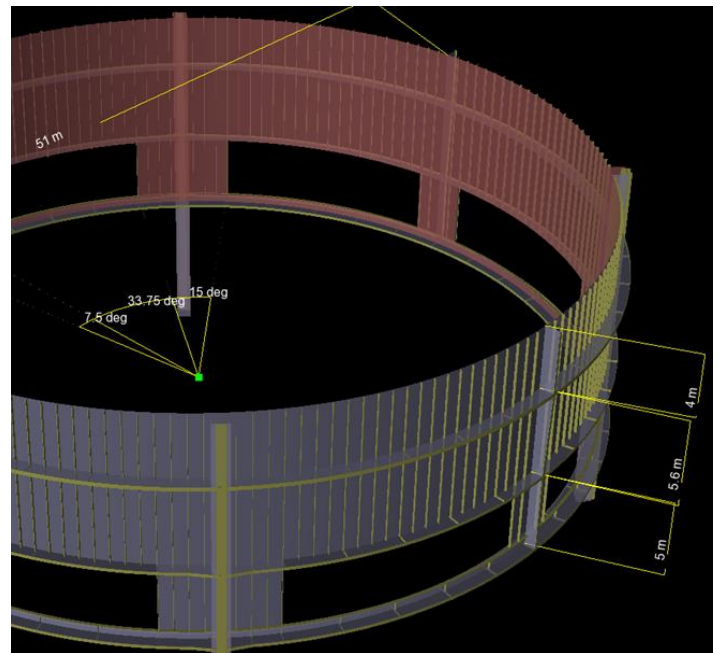

Figure 29 Test steel cage

REFERENCES

Aquastructures(2003)"Havari Laksefjord" (in norwegian). Report no. 2003-132. Aquastructures, Kjøpmannsgata 21 7013 Trondheim. www.aquastructures.no.

Aquastructures(2005) "Teknisk vurdering av anlegg, Tustna kommune" (in norwegian). Report no. HR-300083-103, Aquastructures, Kjøpmannsgata 21 7013 Trondheim. www.aquastructures.no..

Aquastructures (2012) "Verification and Benchmarking of AquaSim,a Softwaretool for Simulation of Flexible Offshore Facilities Exposed to Environmental and Operational Loads. Aquastructures report no. 2012-1755-1. Aquastructures, Kjøpmannsgata 21 7013 Trondheim. www.aquastructures.no.

Aquastructures (2018) "THE AQUASIM PACKAGE THEORY USER MANUAL" TR-30000-2049-2018 02.01.2018. Aquastructures, Kjøpmannsgata 21 7013 Trondheim. www.aquastructures.no.

Babarit, A., & Delhommeau, G. (2015, September): "Theoretical and numerical aspects of the open source BEM solver NEMOH". In 11th European Wave and Tidal Energy Conference (EWTEC2015).

Berstad, A. J., Tronstad, H., Ytterland, A. (2004)" Design Rules for Marine Fish Farms in Norway. Calculation of the Structural Response of such Flexible Structures to Verify Structural Integrity." Proceedings of OMAE2004 23rd International Conference on Offshore Mechanics and Arctic Engineering June 2004, Vancouver, Canada. OMAE2004-51577

Berstad, A. J. and H. Tronstad (2007) "Development and design verification of a floating tidal power unit" OMAE 2007, The 26th International Conference on Offshore Mechanics and Arctic Engineering San Diego, California, 10-15 June, 2007. Paper 29052.

Berstad, A.J. and H. Tronstad (OMAE 2008) "Use of Hydroelastic Analysis for Verification of Towed equipment for Aquisition of Seismic Data" Proceedings of OMAE2008 27th International Conference on Offshore Mechanics and Arctic Engineering June 15-20 2008 Estoril, Portugal OMAE2008-57850

Berstad A. J., L F. Heimstad and J. Walaunet (2014) "Model Testing of Fish Farms for Validation of Analysis Programs" Proceedings of the ASME 2014 33th International Conference on Ocean, Offshore and Arctic Engineering OMAE2014 June 8-13, 2014, San Francisco, California OMAE2014-24647.

Berstad, A.J., J. Walaunet and L. F. Heimstad (2012) "Loads From Currents and Waves on Net Structures" Proceedings of the ASME 2012 31st International Conference on Ocean, Offshore and Arctic Engineering OMAE2012 July 1-6, 2012, Rio de Janeiro, Brazil OMAE2012-83757

Eggen, T.E. (2000) "Buckling and geometrical nonlinear beam-type analyses of timber structures" PhD Thesis Institute of civil engineering NTNU.

Faltinsen, Odd M. (1990) "Sea loads on ships and offshore structures." Cambridge university press ISBN 0 521 37285 2

Sintef (2017) "AquaTraz. Model tests" Report no. OC2017 F-190. Auth. Ivar Nygaard. Sintef Ocean Postboks 4762 Torgården 7465 Trondheim.

Morison, J. R., M.P. O'Brien, J.W. Johnson and S.A. Schaaf (1950), "The Force Exerted by Surface Waves on Piles," *Petroleum Transactions,* AIME. Vol. bold 189, 1950, 149-154

NS 9415(2009) Marine fish farms, Requirements for design, dimensioning, production, installations and operation. Pronorm. Postboks 252, 1326 Lysaker.

Parisella, G. & Gourlay, T.P. (2016): "Comparison of open-source code Nemoh with Wamit for cargo ship motions in shallow water" (2016-23). Faculty of Marine Technology (NTNU), Curtin University.